PERGAMON

Chaos, Solitons and Fractals 15 (2003) 743–760

CHAOS
SOLITONS & FRACTALS

www.elsevier.com/locate/chaos

Homoclinic bifurcations in heterogeneous market models

Ilaria Foroni, Laura Gardini *

Istituto di Scienze Economiche, University of Urbino, 61029 Urbino, Italy

Accepted 5 June 2002

Abstract

We analyze a class of models representing heterogeneous agents with adaptively rational rules. The models reduce to noninvertible maps of R^2. We investigate particular kinds of homoclinic bifurcations, related to the noninvertibility of the map. A first one, which leads to a strange repellor and basins of attraction with chaotic structure, is associated with simple attractors. A second one, the homoclinic bifurcation of the saddle fixed point, also associated with the foliation of the plane, causes the sudden transition to a chaotic attractor (with self-similar structure).

1. Introduction

In the recent literature, several economic models have been proposed to model economies with heterogeneous agents, see for example [4–7,9,10,16]. Most of these heterogeneous agents models describe systems where two typical agents are present: a first group (fundamentalists or arbitrageurs) who believe that the security price is determined by the market fundamental values, and a second group (chartists or technical analysts) who predict the future price by using simple technical trading rules, observing the past prices. Following this stream, we investigate the dynamic behaviour of a class of models representing two groups in which the fractions of agents of each group change according to the mechanism proposed in [5]. One group represents the fundamentalists, while the other group uses the past realizations in a standard adaptive learning mechanism, and the dynamics are governed by a two-dimensional noninvertible map. As the recent literature has emphasized, heterogeneity and learning may lead to market instability and complicated dynamics, and we also find these aspects in our models. That is, the dynamic behaviours may be, as expected, regular (equilibrium and stable cycles) or chaotic. Object of the present work is to investigate the main routes to complex behaviours in the attracting sets and global bifurcations (homoclinic bifurcations) both in the attracting sets and in their basins of attraction. The importance of the homoclinic bifurcations in understanding the dynamics in chaotic regimes has been addressed to the attention of applied economists only recently, mainly in [5,11,12], associated with the dynamics of invertible nonlinear systems. The model we present in this paper gives us the opportunity to extend the application of this important analytical tool also to noninvertible maps (see also [8]). We shall see how the foliation of the phase-space may be involved in the construction of the stable set of saddles (which are determined by taking all the preimages of a local segment). Moreover, we shall see that such bifurcations may be associated with two kinds of complex structures, either in the invariant sets which give the boundary of basins of attraction (thus leading to complex structures in the basins) or in the invariant attracting set (thus leading to a chaotic attracting set, or strange attractor).

The plan of the work is as follows. In Section 2 we shall describe the model. We shall see how assuming that the chartists use an adaptive rule in their forecasts, a two-dimensional noninvertible map, called T_2, is obtained. In Section 3 we shall describe the main features of this two-dimensional map T_2: its foliation and the role played by the two distinct

* Corresponding author. Tel.: +39-722-2586; fax: +39-722-327655.
E-mail address: gardini@uniurb.it (L. Gardini).

0960-0779/03/$ - see front matter
PII: S0960-0779(02)00176-5

inverses of the map. As we shall see, the fixed point is unique and very particular, because a whole line of points is mapped by T_2 into the fixed point. This feature denotes a particular kind of dynamics associated with the inverses (related to sets called focal points and prefocal sets in [2,3], whose role is evidenced in Section 3.4. In Section 3.1 the foliation of T_2 is described, which helps us in the determination of the stable set $W^S(S^*)$ of the saddle fixed point S^*, described in Section 3.2. In Section 3.3 we shall see the homoclinic bifurcation of a saddle set, made up of two cycles, due to the existence of heteroclinic points connecting the first to the second one, and the second one to the first (also called transverse cyclical heteroclinic connection). Associated with such homoclinic orbits there is an invariant Cantor set (with infinitely many repelling cycles), on which the dynamics is chaotic, which constitutes a strange repellor. That is, it is not embedded in some chaotic area or absorbing region. Instead, it belongs to the frontier of the basins of simple attractors (two cycles of T_2), thus leading to a complex structure in the basins of attraction. On the other hand, in Section 3.4 we shall see the sudden transition to a chaotic attractor due to the homoclinic bifurcation of the saddle fixed point S^*. The relevance of the phase-space region in order to have meaningful trajectories, called feasible region, is described in Section 3.5, where we point out that bifurcations may occur also in that region, due to the foliation of T_2.

2. The heterogeneous market model

We consider a cobweb model where $D(p)$ and $S(p)$ are the market demand and supply functions of a nonstorable good. At a given time t, $D(p)$ depends on the current price p_t whereas $S(p)$ depends on the price p_t^e expected by producers at the time in which they decided their production. So, if the production delay is taken as the time unit, the market clearing condition becomes $D(p_{t+1}) = S(p_{t+1}^e)$ and assuming that $D(p)$ is a continuous and decreasing function (hence invertible) the law of motion of the market clearing price is $p_{t+1} = D^{-1} \circ S(p_{t+1}^e)$. We consider the simplest case in which D is a linear function, say $D(p_t) = A - Bp_t$, with $A > 0$ and $B > 0$, and for the supply function we assume that producers maximize the net profit obtaining $S(p_{t+1}^e) = bp_{t+1}^e$ with $b > 0$, so that we get

$$p_{t+1} = D^{-1} \circ S(p_{t+1}^e) = \frac{A - bp_{t+1}^e}{B}$$

and we have to specify the formation of the expected value for the time $(t+1)$, estimated on the basis of the information set at time t, say $\vec{P}_t$, i.e. $p_{t+1}^e = H(\vec{P}_t)$.

Following the approach of Adaptive Belief Systems developed in [4,7] (see also [13], to which we refer for a detailed description of the model), we consider the equilibrium price dynamics in the cobweb model with heterogeneous beliefs where agents can choose between two different predictors H_1 and H_2. The fractions $n_{j,t}$ (with $j = 1, 2$) of agents using predictor H_j in period t can change over time. The updated fraction $n_{j,t+1}$ of agents using predictor H_j in the next period is $n_{j,t+1} = (\exp(\beta U_{j,t+1})/Z_{t+1})$ for $j = 1, 2$; where $Z_{t+1} = \sum_{j=1}^{2} \exp(\beta U_{j,t+1})$ and the performance measure $U_{j,t+1}$ for predictor H_j is given below, so that the fractions $n_{1,t+1}$ and $n_{2,t+1}$ add up to 1 and the parameter β is the intensity of choice measuring how fast agents switch predictors. We get:

$$\begin{aligned} p_{t+1} &= n_{1,t} D^{-1} \circ S_1(H_1(\vec{P}_t)) + n_{2,t} D^{-1} \circ S_2(H_2(\vec{P}_t)) = n_{1,t}\left(\frac{A - bH_1(\vec{P}_t)}{B}\right) + n_{2,t}\left(\frac{A - bH_2(\vec{P}_t)}{B}\right) \\ n_{j,t+1} &= \frac{\exp(\beta U_{j,t+1})}{Z_{t+1}}; \quad j = 1, 2 \end{aligned} \tag{1}$$

where

$$U_{j,t+1} = p_{t+1} bH_j(\vec{P}_t) - \frac{bH_j^2(\vec{P}_t)}{2} - C_j; \quad j = 1, 2$$

and C_j are positive constants. In order to close the model we introduce the predictor mechanisms H_1 and H_2, which differ from the examples quoted in the literature of *Adaptively Rational Equilibrium Dynamics* models. We suppose that the components of the first group are a kind of fundamentalists and believe that the prices would go back to their fundamental value. To estimate the equilibrium price they know the demand and supply functions, and solving the equation $A - Bp_t = bH_1(\vec{P}_t)$ at equilibrium, that is $A - Bp^* = bp^*$, they obtain the result

$$p^* = \frac{A}{b + B} \tag{2}$$

so that the first predictor becomes

$$H_1(\vec{P}_t) = p^* \tag{3}$$

The second group of producers uses a standard adaptive learning mechanism with speed of adjustment α of the form

$$H_2(\vec{P}_t) \equiv p^e_{t+1} = (1-\alpha)p^e_t + \alpha p_t \tag{4}$$

With our assumptions we have $U_{1,t+1} = \frac{b}{2}p^*(2p_{t+1} - p^*) - C_1$ and $U_{2,t+1} = \frac{b}{2}p^e_{t+1}(2p_{t+1} - p^e_{t+1}) - C_2$, and we always assume $C_1 > C_2 > 0$ (as H_2 is a less sophisticated predictor than H_1). The updated fractions of agents, after observing the realized price p_{t+1} are

$$n_{1,t+1} = \frac{\exp\left[\beta\left(\frac{b}{2}p^*(2p_{t+1} - p^*) - C_1\right)\right]}{Z_{t+1}} \tag{5}$$

$$n_{2,t+1} = \frac{\exp\left[\beta\left(\frac{b}{2}p^e_{t+1}(2p_{t+1} - p^e_{t+1}) - C_2\right)\right]}{Z_{t+1}} \tag{6}$$

with $n_{1,t} + n_{2,t} = 1\ \forall t$ and we have

$$p_{t+1} = \frac{A}{B} - n_{1,t}\left(\frac{bp^*}{B}\right) - n_{2,t}\left(\frac{bp^e_{t+1}}{B}\right) \tag{7}$$

$$p^e_{t+2} = (1-\alpha)p^e_{t+1} + \alpha p_{t+1} \tag{8}$$

For algebraic convenience we introduce, following [5], the difference

$$m_{t+1} = n_{1,t+1} - n_{2,t+1} \tag{9}$$

so that $m_{t+1} = 1$ when all producers choose H_1 as predictor for the next period, and $m_{t+1} = -1$ in the opposite case. Substituting (5) and (6) in (9) we get

$$m_{t+1} = \frac{\exp(\beta U_{1,t+1}) - \exp(\beta U_{2,t+1})}{\exp(\beta U_{1,t+1}) + \exp(\beta U_{2,t+1})} \tag{10}$$

so that

$$m_{t+1} = \tanh\left(\frac{\beta}{2}(U_{1,t+1} - U_{2,t+1})\right) \tag{11}$$

or

$$m_{t+1} = \tanh\left(\frac{\beta}{2}\left[\frac{b}{2}p^*(2p_{t+1} - p^*) - C_1 - \frac{b}{2}p^e_{t+1}(2p_{t+1} - p^e_{t+1}) + C_2\right]\right) \tag{12}$$

By the relation

$$n_{1,t+1} = \frac{1+m_{t+1}}{2} \quad \text{and} \quad n_{2,t+1} = \frac{1-m_{t+1}}{2} \tag{13}$$

we obtain the dynamic model

$$\begin{cases} p_{t+1} = \dfrac{A}{B} - \dfrac{1+m_t}{2}\left(\dfrac{bp^*}{B}\right) - \dfrac{1-m_t}{2}\left(\dfrac{bp^e_{t+1}}{B}\right) \\ m_{t+1} = \tanh\left(\dfrac{\beta}{2}\left[\dfrac{b}{2}p^*(2p_{t+1} - p^*) - C_1 - \dfrac{b}{2}p^e_{t+1}(2p_{t+1} - p^e_{t+1}) + C_2\right]\right) \\ p^e_{t+2} = (1-\alpha)p^e_{t+1} + \alpha p_{t+1} \end{cases} \tag{14}$$

We introduce the following change of variables

$$X = p - p^* \quad \text{and} \quad X^e = p^e - p^* \tag{15}$$

where p^* is the equilibrium price estimated in (2). However, instead of writing the new system in the new coordinates X_t and X^e_t, for the sake of simplicity of notation, we maintain the old formulation of p_t and p^e_t which henceforth denote the deviations from the equilibrium price. The new system reads as

$$\begin{cases} p_{t+1} = -\dfrac{1-m_t}{2}\left(\dfrac{bp^e_{t+1}}{B}\right) \\ m_{t+1} = \tanh\left(\dfrac{\beta}{2}\left[-\dfrac{b}{2}p^e_{t+1}(2p_{t+1} - p^e_{t+1}) + C_2 - C_1\right]\right) \\ p^e_{t+2} = (1-\alpha)p^e_{t+1} + \alpha p_{t+1} \end{cases} \tag{16}$$

which, by substituting the first equation in the other two, can be expressed as a two-dimensional map, say T_2, in the variables (z_t, m_t) with $z_t = p^e_{t+1}$:

$$T_2 : \begin{cases} z_{t+1} = z_t\left[(1-\alpha) - \alpha\dfrac{b(1-m_t)}{2B}\right] \\ m_{t+1} = \tanh\left[\dfrac{\beta b}{4}z_t^2\left(\dfrac{b(1-m_t)}{B}+1\right) + \dfrac{\beta}{2}(C_2 - C_1)\right] \end{cases} \tag{17}$$

3. The dynamics of the map T_2

In this section we shall consider the dynamics of the economic model described by the map T_2, in order to investigate the structure of attracting sets and of their basins of attraction. We shall see that many particular homoclinic bifurcations which occur are related with the structure of the foliation of the noninvertible map. We shall first describe this in Section 3.1. Then we shall see the structure of the stable set of the unique fixed point saddle, and the transition to complex structure in the phase-space associated with simple attractors, due to cyclical heteroclinic orbits which play the same role as homoclinc bifurcations of saddle cycles. A peculiar homoclinic bifurcation of the saddle fixed point is described after, causing the sudden transition to a chaotic attractor (with fractal structure). Finally, some comments on the feasible region in the phase-plane are necessary, in order to have suitable applications of the model.

3.1. General properties

Let us rewrite the map T_2 given in (17) by using the symbol "′" to denote the unit time advancement operator, obtaining

$$T_2 : \begin{cases} z' = z\left[(1-\alpha) - \alpha\dfrac{b}{2B}(1-m)\right] \\ m' = \tanh\left[\dfrac{\beta b}{4}z^2\left(\dfrac{b(1-m)}{B}+1\right) + \dfrac{\beta}{2}(C_2 - C_1)\right] \end{cases} \tag{18}$$

The map is defined in the whole plane and has only one fixed point, S^*, given by

$$S^* = (z^*, m^*) = \left(0, \tanh\left[\frac{\beta}{2}(C_2 - C_1)\right]\right) \tag{19}$$

We notice that as the hyperbolic tangent assumes values in the interval $(-1,1)$ the image of a point $(z,m) \in \Re^2$ always belongs to the strip of the plane with $m \in (-1,1)$. Furthermore the map T_2 is noninvertible, this means that even if a point (z,m) has a unique image under the application of T_2, the backward iteration of T_2 is not uniquely defined. Given a point (z',m') with $m' \in (-1,1)$ its rank-1 preimages are obtained by solving the algebraic systems in (18) and we get

$$T_{2_1}^{-1} \begin{cases} z = \dfrac{z'}{2-\alpha} + \sqrt{\dfrac{z'^2}{(2-\alpha)^2} + \dfrac{4\alpha}{\beta b(2-\alpha)}\left[\operatorname{arctanh}(m') - \dfrac{\beta}{2}(C_2 - C_1)\right]} \\ m = 1 + \dfrac{2B}{\alpha b}\left(\dfrac{z'}{z} - 1 + \alpha\right) \end{cases} \tag{20}$$

$$T_{2_2}^{-1} \begin{cases} z = \dfrac{z'}{2-\alpha} - \sqrt{\dfrac{z'^2}{(2-\alpha)^2} + \dfrac{4\alpha}{\beta b(2-\alpha)}\left[\operatorname{arctanh}(m') - \dfrac{\beta}{2}(C_2 - C_1)\right]} \\ m = 1 + \dfrac{2B}{\alpha b}\left(\dfrac{z'}{z} - 1 + \alpha\right) \end{cases} \tag{21}$$

assuming that the discriminant, say Δ, in the above expressions is positive. So, if $\Delta > 0$, a point (z',m') has two real preimages given by $T_2^{-1}(z',m') = T_{2_1}^{-1}(z',m') \cup T_{2_2}^{-1}(z',m')$. In the case $\Delta < 0$ the point (z',m') has no preimages. Following [19] we say that the plane is divided into two regions, called Z_2 and Z_0, whose points have two or zero preimages respectively. These two regions are separated by the curve of equation $\Delta = 0$, that is:

$$m = \tanh\left(-\frac{\beta b}{4\alpha(2-\alpha)}z^2 + \frac{\beta}{2}(C_2 - C_1)\right) \tag{22}$$

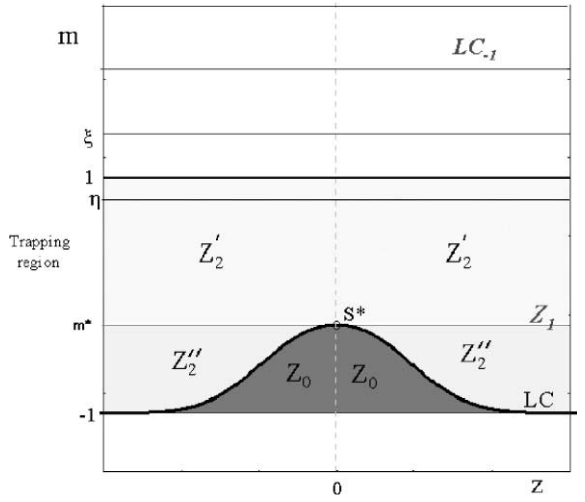

Fig. 1. $Z_2 = Z_2' \cup Z_2''$.

called critical curve LC. The points belonging to LC have two coincident rank-1 preimages located on the line LC_{-1} given by

$$LC_{-1}: \quad m = 1 + \frac{2B}{\alpha b} \tag{23}$$

The curves LC and LC_{-1} are represented in Fig. 1 (LC separates the region Z_0 from Z_2). The curve LC_{-1} can also be obtained looking for the locus of points in which the determinant of the Jacobian matrix of T_2 vanishes, because $LC = T_2(LC_{-1})$ is a set of points in which the map T_2 is locally noninvertible. Following this procedure we calculate

$$J(z,m) = \begin{bmatrix} J_{11} & J_{12} \\ J_{21} & J_{22} \end{bmatrix}$$

where

$$J_{11} = 1 - \alpha - \frac{\alpha b}{2B}(1-m), \quad J_{12} = z\frac{\alpha b}{2B}$$

$$J_{21} = \left[1 - \tanh^2\left\{\frac{\beta b}{4}z^2\left(\frac{b(1-m)}{B}+1\right) + \frac{\beta}{2}(C_2 - C_1)\right\}\right]\frac{\beta b}{2}z\left[\frac{b}{B}(1-m)+1\right]$$

$$J_{22} = \left[1 - \tanh^2\left\{\frac{\beta b}{4}z^2\left(\frac{b(1-m)}{B}+1\right) + \frac{\beta}{2}(C_2 - C_1)\right\}\right]\left(-\frac{\beta b^2 z^2}{4B}\right)$$

It is worth noting that $\det J = 0$ when $z = 0$ or when $m = 1 + ((2B)/(\alpha b))$. Nevertheless the line $z = 0$ is not a critical line of the usual kind, associated with the foliation of the plane. In fact, we notice that every point of the axis $z = 0$ is mapped by T_2 into a unique point, that is the fixed point $S^* = (0, m^*)$:

$$T_2(0,m) = (0,m^*) \quad \forall m \in \Re \tag{24}$$

From this fact, following [2,3], we argue that at least one inverse of T_2 must be a map with a vanishing denominator. And this is true, as we have seen that the first of the two inverses in (20) has a denominator which vanishes at the points (z', m') satisfying

$$\frac{z'}{2-\alpha} + \sqrt{\frac{z'^2}{(1-\alpha)^2} + \frac{4\alpha}{\beta b(2-\alpha)}\left[\arctan\mathrm{h}(m') - \frac{\beta}{2}(C_2 - C_1)\right]} = 0 \tag{25}$$

that is, for

$$z' < 0 \quad \text{and} \quad m = \tanh\left(\frac{\beta}{2}(C_2 - C_1)\right) = m^* \tag{26}$$

In a similarly way, $T_{2_2}^{-1}$ in (21) has a denominator which vanishes for $z' > 0$ and $m = m^*$.

To summarize, the horizontal line through the fixed point of T_2, $m = m^*$, is a singular line because on its points the denominator of at least one of the inverses vanishes. Moreover, following the definition given in [2,3], the fixed point $(0, m^*)$ is a *focal point* Q' for T_2^{-1} with *prefocal set* δ'_S the line $z = 0$. This example shows an important peculiarity of plane maps: in order to have a "well behaved" fixed point (both for forward and backward iterations) it is not enough to have a point mapped into itself, it is also necessary to have it as a fixed point of at least one of the inverses. This is not the case in our model, the fixed point being the focal point Q' for both the two distinct inverses of T_2^{-1}. As $m = m^*$ is a singular line for the inverse T_2^{-1}, the foliation of the plane assumes a new particular structure. From the definition of T_2 it follows that the points of the plane with

$$m > \xi \quad \text{where} \quad \xi = \left(1 + \frac{B}{b}\right) > 1 \tag{27}$$

are mapped into a point with $m' < 0$. In particular, the line $m = \xi$ is mapped in $m = m^*$, that is, the singular line of the inverse. Note the particular role played by this line in the foliation: a point (z, m^*) has only one real preimage on the line $m = \xi$, the other being at infinity (for this reason we have denoted it by Z_1 in Fig. 1). This identifies a region of the range of T_2, denoted by Z_2'' in Fig. 1, included between the curve LC and the line $m = m^*$. The points $(z', m') \in Z_2''$ have two distinct inverses, the first one is placed between $m = \xi$ and LC_{-1} ($m = 1 + ((2B)/(\alpha b))$) the second one is located above LC_{-1}. The remaining region of Z_2 (belonging to the strip delimited by $m = m^*$ and $m = 1$), denoted by Z_2', is a trapping region because every point belonging to Z_2' is mapped in the same region, i.e. $T_2(Z_2') \subset Z_2'$. So Z_2' is the region containing the attractors and the ω-limit sets of T_2. We notice that in Z_2 the line of equation

$$m = \eta \quad \text{with} \quad \eta = 1 - \frac{2B}{\alpha b}(1 - \alpha) < 1$$

is mapped into the vertical axis $z = 0$, which is in turn mapped in the fixed point S^*. Hence the stable set of S^* always include the lines $z = 0$ and $m = \eta$. Moreover the image of $m = \eta$ through T_2 is folded up in the point S^* therefore the segment of axis $z = 0$ with $m \in (m^*, 1)$ is covered by a double segment of images of the points (z, m) belonging to $m = \eta$. Stated in other words, every point $(0, m')$ with $m^* < m' < 1$ has two distinct preimages on the line $m = \eta$, symmetrical with respect to $z = 0$. Finally, it is simple to verify that every point $(z', m') \in Z_2'$ has two distinct inverses that are located one on the right, and one on the left, of the prefocal curve δ'_S, $z = 0$, and at the same time one of the preimages is located above the line $m = \eta$, and the other under the same line. These facts lead to an unusual foliation of the map T_2, due to the presence of an inverse with focal point. This particular kind of foliation allows us to explain the bifurcations of the attractors and their basins of attraction. First of all we notice that

$$T_2(-z, m) = (-z', m')$$

i.e. the images of points symmetrical with respect to the vertical axis $z = 0$ are also symmetrical with respect to the same line. Then we can write the following:

Proposition 1. *An invariant attracting set of the map T_2 is symmetric with respect to $z = 0$, or it coexists with an invariant attracting set symmetric with respect to it, and it is placed in the region $m^* < m < 1$.*

3.2. Fixed point and its stable set

We shall investigate the dynamics of the map T_2 as the *switching coefficient* β increases. To simplify the exposition we fix the values of the other parameters:

$$C_1 = 15, \quad C_2 = 5, \quad \alpha = 0.8, \quad b = 1.35, \quad B = 0.5, \quad A = 15 \tag{28}$$

the dynamics of the model being similar for different constellations of the economic parameters. For low values of β, the fixed point S^* of T_2 is stable and globally attracting. Because of the complexity of the expression of T_2, it is not possible to investigate analytically the local stability as a function of the parameters of the models. We have numerically computed the eigenvalues of the Jacobian matrix in $S^* = (0, m^*)$, $J(S^*)$. We already know that $\det J(S^*) = 0$ and this means that $J(0, m^*)$ always has one eigenvalue equal to zero, which corresponds to the eigenvector along the line $z = 0$. We recall that every point of the vertical axis is mapped into S^* after one iteration of the map T_2. As β increases we have observed that the other eigenvalue goes towards -1 and for $\beta \simeq 0.023$ the system undergoes a flip bifurcation with the consequent birth of an attracting cycle of period 2. The cycle is composed of two points $\{x_1, x_2\}$, symmetrically placed with respect to $z = 0$. In this case the use of T_2^2, double iterate of T_2, is more convenient to understand the dynamics of the model and, in particular, we are interested in the structure of the stable set of S^* which is now unstable (a saddle). In

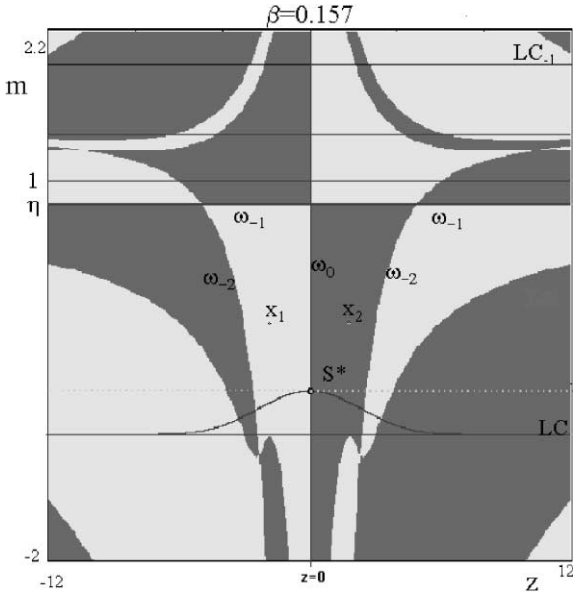

Fig. 2. The frontier denotes the stable set of the saddle S^*, $W^S(S^*)$.

Fig. 2 we show the two points $\{x_1, x_2\}$ that are at the same time a 2-cycle for the map T_2 and two fixed points for the iterated T_2^2. We consider the basin of attraction of x_1 and x_2 under T_2^2, $\mathscr{B}(x_1)$ and $\mathscr{B}(x_2)$ respectively, that is, the initial conditions which converge to x_1 or x_2 under the iteration of the map T_2^2. Even if the basins are symmetrical with respect to $z = 0$ their structures are not simple. We must determine the frontier

$$\mathscr{F} = \partial\mathscr{B}(x_1) = \partial\mathscr{B}(x_2)$$

that separates the two basins. Such a frontier behaves as a repelling set for the points near it, since it acts as a watershed for the trajectories of the map T_2^2. Points belonging to $\mathscr{F}$ are mapped into $\mathscr{F}$ both under forward and backward iteration of T_2^2: that is $T_2(\mathscr{F}) \subseteq \mathscr{F}$, $T_2^{-1}(\mathscr{F}) = \mathscr{F}$. This implies that if a saddle point belongs to $\mathscr{F}$, then $\mathscr{F}$ must also contain the whole stable manifold. We consider the local stable manifold of the saddle point S^*, which is the line $z = 0$. This line, called ω_0 in Fig. 2, behaves as a repelling line, because the unstable manifold of the saddle S^* has a branch pointing toward x_1 and the opposite branch going toward x_2. The other parts of the frontier $\mathscr{F}$ can be obtained by taking all the preimages of the local stable set, that is, we have

$$\mathscr{F} = W^S(S^*) = \bigcup_{n \geqslant 0} T_2^{-n}(\omega_0)$$

where T_2^{-n} represents the set of all the rank-n preimages. Fig. 2 shows the basins of attractions $\mathscr{B}(x_1)$ and $\mathscr{B}(x_2)$ in two different colors, and $\mathscr{F}$ is the boundary separating the two basins. We want to stress that for T_2 the 2-cycle $\{x_1, x_2\}$ is nearly globally attracting since only the points belonging to $W^S(S^*)$ do not converge to it. However, in this way we have investigated the stable set of the saddle fixed point S^*, and this is important in order to understand the homoclinic bifurcations involving the fixed point. As we shall see, the structure of the stable set of S^* changes a little from that shown in Fig. 2, as β is increased, due to global bifurcations involving the foliation of the map. In fact, as β increases the 2-cycle becomes unstable via a Neimark–Sacker–Hopf bifurcation (see [17]) which leads to the birth of two attracting closed invariant curves around x_1 and x_2. The invariant curves together form a unique attracting invariant set of T_2. For the map T_2^2 the closed curves, say Γ_1 and Γ_2, represent two coexistent attracting sets and we can determine, as before, their basins of attraction for T_2^2. The frontier is still

$$\mathscr{F} = \partial\mathscr{B}(\Gamma_1) = \partial\mathscr{B}(\Gamma_2) = W^S(S^*)$$

The two basins depicted in Fig. 3 have now a more complex structure, generated by a global bifurcation called *tangent bifurcation* between an invariant set, the basin boundary, and the critical curve LC. We notice that the regions A and A' indicated by the arrows in Fig. 3 (due to portions of basins previously, in Fig. 2, located in the region Z_0 and therefore without preimages) are now crossing LC (see the enlargement). This means that the pieces of A and A' crossing LC now

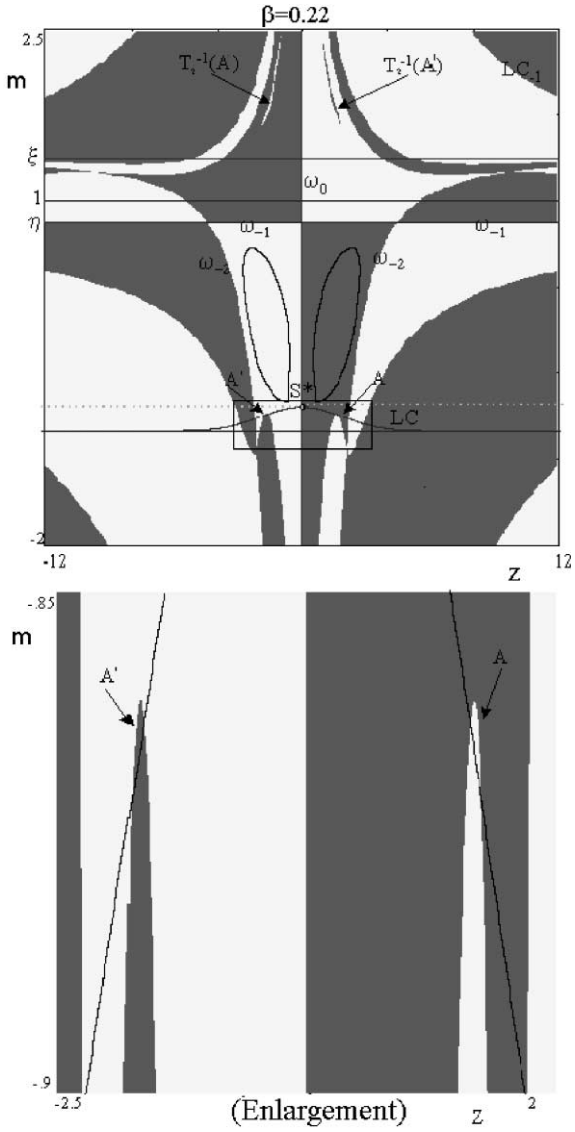

Fig. 3. Bifurcation of the saddle set $W^S(S^*)$.

belong to Z_2''. Their preimages give rise to new structures called holes, or islands, of a basin inside the other one (see [18,19]). In fact, considering as an example the region A, its preimage is formed by

$$T_2^{-1}(A) = T_{2_1}^{-1}(A) \cup T_{2_2}^{-1}(A)$$

which is a "connected island" (crossing LC_{-1}) of a basin (the light grey one in Fig. 3) inside another (dark grey one in Fig. 3). In a symmetrical way, the same mechanism works for $T_2^{-1}(A')$. As β increases, the two portions A and A' in Z_2'' grow up and reach the horizontal line $m = m^*$ (singular line for the inverse). At the moment of the contact of A and A' with $m = m^*$, the first component of the inverses has a contact with the line $m = \xi$, the second has a contact with Poincaré equator at infinity. This gives rise, increasing β when A and A' cross $m = m^*$ and enter Z_2', to the appearance of other portions of the basins on the opposite side of the plane, and this can been seen in Fig. 4 (tongues evidenced by the arrows). Clearly as β increases further these new tongues from the region Z_0 will have a contact with the critical curve LC, entering the region Z_2'', that is: the same mechanism described above is repeated, giving rise to the appearance of other holes and tongues. We note that in Fig. 4 the attractors are changed, the map T_2 possess two distinct (and symmetrical) cycles of period 12. However, the two colors in Fig. 4 do not have the meaning of basins, they have been

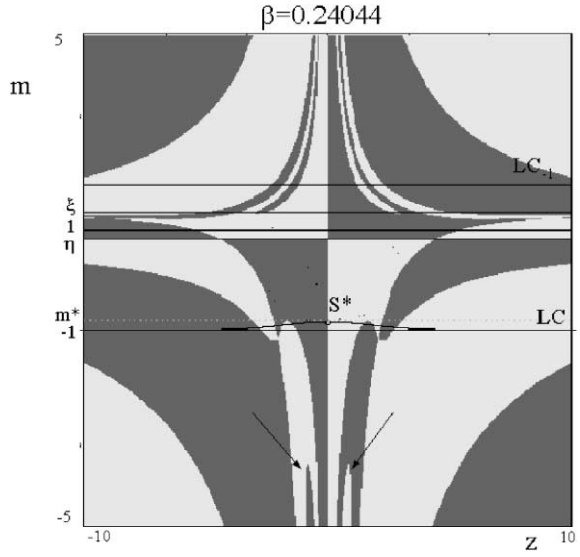

Fig. 4. Further changes of $W^S(S^*)$.

used only to emphasize their frontier which is the stable set $W^S(S^*)$ of the saddle S^*, and the contact bifurcations described above are to be interpreted, for the map T_2, as global bifurcations which change the structure of the stable set of the saddle S^*.

3.3. Homoclinic bifurcations leading to strange repellors

We have seen in Fig. 4 that on the invariant set $\Gamma = \Gamma_1 \cup \Gamma_2$ there are quasi periodic trajectories which are dense in the invariant set. As often occurs after a Neimark–Hopf bifurcation, as β grows up situations of quasiperiodicity are followed by "periodic windows" that are opened and closed via saddle-node bifurcations. On the invariant set Γ two cycles, a saddle and a node appear, and the unstable manifold of the saddle is composed by arcs of invariants curves connecting the saddle with the node. This situation leads to the existence of a closed invariant curve made up of a *saddle-node connection* (see the qualitative picture in Fig. 5). In these cases the invariant curve Γ continue to exist, and it is the closure of the unstable manifold of the saddle cycle, even if the generic trajectory converges to the attracting node. We notice that Γ is also an *invariant attracting set.* Moreover, if we consider the points which converge toward one of the three points of the cycle for the third iterate, the stable manifolds of the saddles give the frontier of the basins of attraction, as depicted in the qualitative Fig. 5b. In our model an unusual situation occurs, due to the symmetry of the map T_2. On the closed curve $\Gamma = \Gamma_1 \cup \Gamma_2$, attracting for T_2, two saddle-node bifurcations occur at the same time giving rise to two attracting 6-cycles and two 6-cycles of saddle type. These two cycles saddles and nodes are, of course, symmetrical with respect to the vertical axis $z = 0$. When two coexisting attractors exist, some points converge to the first attractor and some other converge toward the second one. In Fig. 6 we show one of the two symmetrical attracting 6-cycles. The points which are coloured in dark grey go toward the cycle which is represented in the picture, the light grey ones approach the other cycle. We recall that the stable set $W^S(S^*)$ (a set of points of zero measure) which converge to S^* always exists and even if it is not clear in the figure, it has the same structure that we have previously seen in the Figs. 2–4. We also notice that the invariant curve $\Gamma_1 \cup \Gamma_2$ depicted in Fig. 2 still exists, but we cannot see it because we are in a "periodic window". Due to the symmetry, the invariant curve has a peculiar structure being formed by both the saddle cycles, i.e. Γ is an heteroclinic connection composed of the unstable manifolds of two 6-cycles of saddle type. Let us denote by $N = \{N_1, \ldots, N_6\}$ one 6-cycle node and by $S = \{S_1, \ldots, S_6\}$ the related saddle. The symmetrical ones are denoted by $N' = \{N'_1, \ldots, N'_6\}$ and $S' = \{S'_1, \ldots, S'_6\}$. In the qualitative Fig. 7 we show the mechanism which occurs in our case. Because of the symmetry of the map T_2, it suffices to consider what happens in one half plane, $z < 0$, for example. As it can be seen from Fig. 7, the stable manifolds of the saddles S and S' form the boundary of the basins of attractions: the dark grey points converge toward one of the attracting cycle the light grey ones go toward the symmetrical cycle. For sake of simplicity we denote by s the invariant set which represents the union of the two saddles (i.e. $s = S \cup S'$) so also s is an invariant set of saddle type. Thus, what is represented in Fig. 6 is the frontier

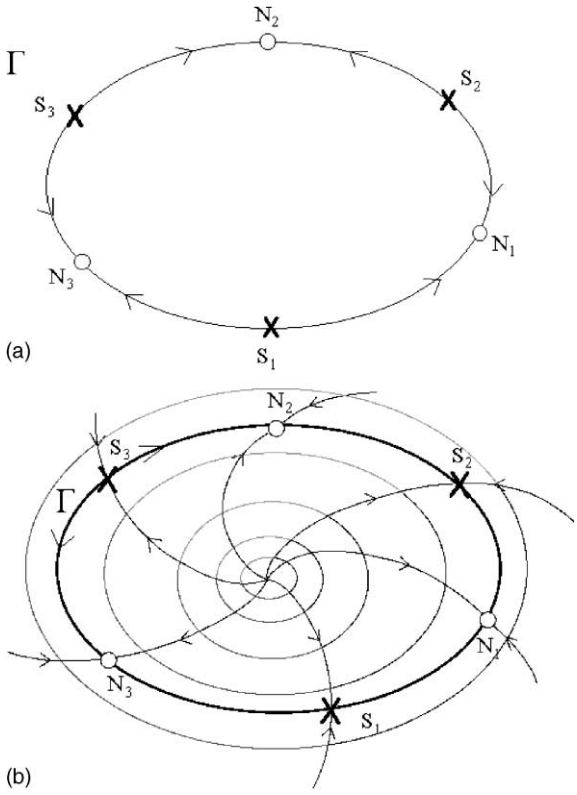

Fig. 5. Qualitative picture of a saddle-node connection in (a). Qualitative representation of basins for the iterated map, issuing from a repelling focus in (b).

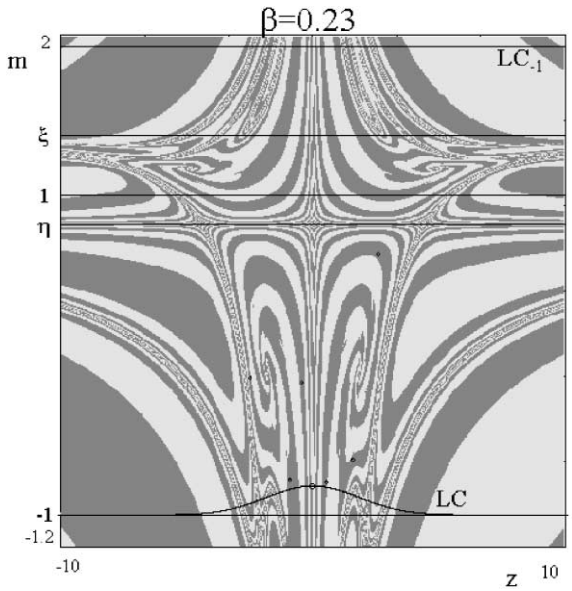

Fig. 6. Basins of attractors of two symmetric 6-cycles of the map T_2.

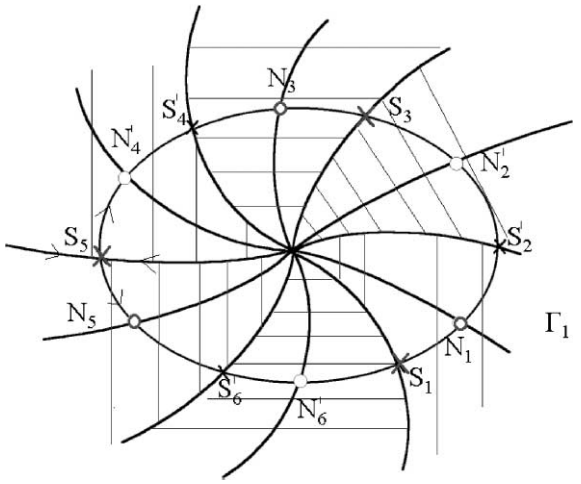

Fig. 7. Qualitative representation of the structure of the closed curve Γ_1. The other points of the 6-cycle belong to the symmetric curve Γ_2.

$$\mathscr{F} = \partial\mathscr{B}(N) = \partial\mathscr{B}(N') = W^S(S) \cup W^S(S') = W^S(s) \tag{29}$$

The basin structure is not complex (as it may seem at a first glance) the light grey and dark grey spirals in the figure, issuing from the points x_1 and x_2 belonging to the unstable 2-cycle of focus type have $W^S(S^*)$ as limit set. Moreover some islands can appear in the basins due to the mechanisms that we have explained above. If we repeatedly enlarge the figure, we will see that the arcs which form $\mathscr{F} = W^S(s)$ are smooth and we notice that there are not contacts or intersections between $W^U(s)$ (whose limit set includes Γ) and the boundary of the basins $\mathscr{F} = W^S(s)$. Hence the saddle cycles have no homoclinic points, and this is the usual situation occurring when we are in a periodic window, not far from a Neimark–Hopf bifurcation. Several periodic windows are generally opened and closed, and this mechanism creates a sequence of different regimes: regimes of quasiperiodic trajectories followed by periodic window of cycles of different periods (see [14,17]). This also happens in our model. However here we prefer to deal with a particular global bifurcation, of homoclinic type, associated with the 6-cycle whose basins are shown in Fig. 6. We shall see that this bifurcation will give rise to the birth of a strange repellor and hence to the presence of "unstable chaos", which causes the transition from regular basins of the 6-cycles (as shown in Fig. 6) to complex basins of the 6-cycle (as shown in Fig. 12). This "route to chaos" can be explained by analyzing the basins of attraction of the map T_2. As we have seen in Fig. 6, the structure of the basins is quite regular, and becomes more complicated as β increases, due to qualitative bifurcations of contact type, for which there are "tongues" which come from the region Z_0 and enter in Z_2. Moreover, as β increases from the value of Fig 6 the attractors undergo a flip-bifurcation that generates two attracting nodes of period 12. However, we continue to indicate the new symmetrical attractors with N and N' and we also remark that the invariant closed curve $\Gamma = \Gamma_1 \cup \Gamma_2$ still exists and is formed by the unstable manifolds of all the saddles. In the qualitative picture of Fig. 8 we show the mechanism associated with the flip-bifurcation of the node of period 6. A point of the node (say N_i) becomes a saddle (say $\overline{N}_i$) and in the neighborhood of $\overline{N}_i$ two points of the new 12-cycle appears ($N_{i,1}$ and $N_{i,2}$). As it occurs also before the flip bifurcation, the basin of attraction of every node is bounded by the stable manifolds of the neighboring saddles, that we call in our qualitative picture S_i and S_j, and the invariant curve Γ is made up of the unstable manifolds of all the saddles, that is, $\Gamma = W^U(s)$. We remark that these bifurcations do not change the dynamics of the map T_2 on the boundary $\mathscr{F}$. The restriction of the map T_2 to the invariant set $\mathscr{F}$ is regular, without complex behaviour, as long as $W^S(s) \cap W^U(s) = \emptyset$. However a homoclinic bifurcation, associated with infinitely many unstable periodic points, occurs because of the peculiar structure of the foliation of the map and the existence of the tongues that we have previously described. The homoclinic bifurcation occurs at a value of β in the interval (0.24476, 0.24477). In fact, when $\beta = 0.24476$ there is no intersection between the stable and the unstable manifold of the saddle set s, whereas for $\beta = 0.24477$ the intersections already occurred and an invariant chaotic set exists. In Fig. 9a we show the basins of the two nodes of period 12 before the homoclinic bifurcation, and we notice in the enlargement of Fig. 9b that one arc of the frontier (represented by a light grey tongue between the dark grey points) is approaching the invariant curve Γ. At the moment of the contact a homoclinic bifurcation occurs. In fact, as we can see in the enlargement shown in Fig. 10, after the bifurcation, the light grey arc has crossed Γ and hence has also crossed the unstable manifold of the saddle cycle which form Γ. We recall that the stable manifold of the saddles is given by the frontier of the basins

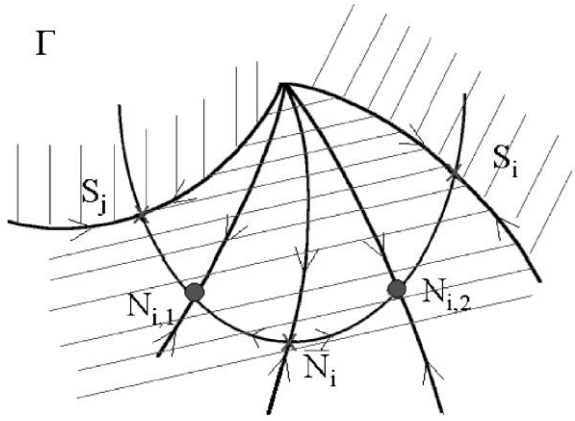

Fig. 8. Qualitative picture of the flip bifurcation of the 6-cycle node.

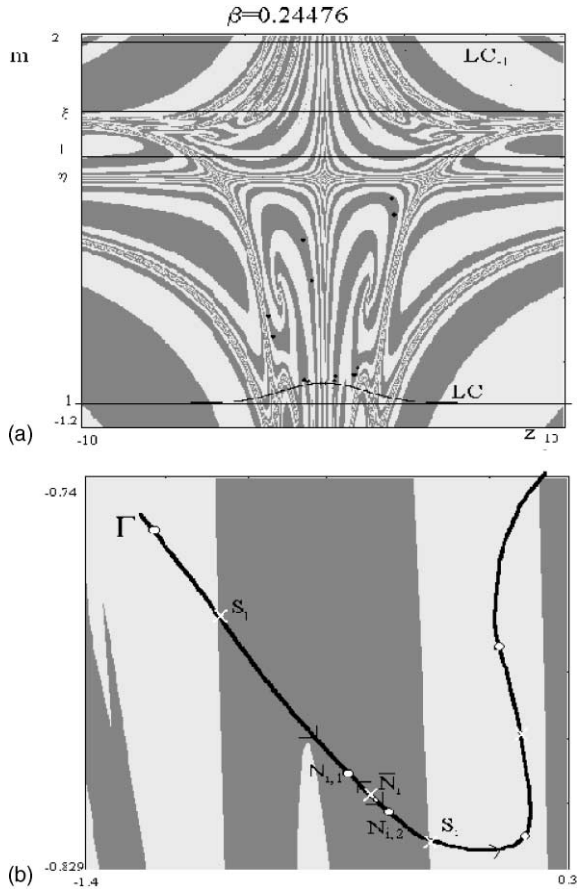

Fig. 9. Basins of the two 12-cycles in (a), enlargement in (b).

of attraction, so that for example the points indicated by p_i and q_i in Fig. 10 belongs at the same time to $W^U(s)$ and $W^S(s)$ and as a consequence p_i and q_i are homoclinic points for s. The preimages of p_i and q_i are infinitely many toward the point S_j, as can be seen from Fig. 10. A similar process occurs, due to the symmetry, for the dark grey arc near the saddle S_i, so that infinitely many dark grey strips also are created inside the light grey tongues showing the self-similar structure that is associated with the homoclinic bifurcation. We notice that this homoclinic bifurcation is also called a

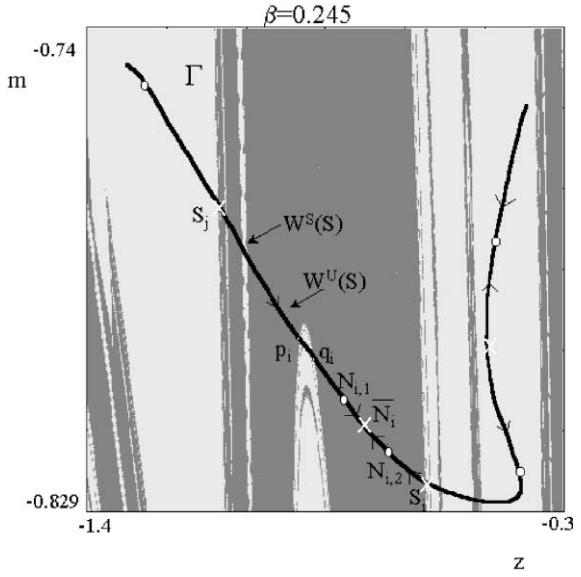

Fig. 10. Transverse intersections between $W^S(s)$ and $W^U(s)$.

cyclical heteroclinic connection in the sense of Birkhoff who first showed that the same properties occur when the stable and unstable manifold of a saddle fixed point intersect transversally, say $W^S(O) \cap W^U(O) \neq \emptyset$ where O is a saddle, or when there are two saddles O and O' and $W^S(O) \cap W^U(O') \neq \emptyset$ giving heteroclinic points, coupled with other heteroclinic points due to $W^U(O) \cap W^S(O') \neq \emptyset$ forming an heteroclinic connection (see also [15]). In such a case, for the saddle set $o = O \cup O'$, due to transverse intersections of $W^U(o) \cap W^S(o) \neq \emptyset$, which are called homoclinic points of *nonsimple type* by Birkhoff and Smith in [1], the same properties occur as for the homoclinic points of saddle fixed point (called by Birkhoff homoclinic points of *simple type*). This kind of homoclinic bifurcation (or cyclical heteroclinic connection) occurs in our model for the saddle cycles of period 6, S and S', giving homoclinic points for the saddle set $s = S \cup S'$. And we recall that the existence of an homoclinic orbit is sufficient to prove the presence of chaotic dynamics because we can demonstrate that in the neighborhood of the homoclinic orbit there are infinitely many repelling cycles and an invariant scrambled set on which the restriction of the map is chaotic in the sense of Li and Yorke (see [20–22]). As β is further increases a reverse flip-bifurcation, or period-halving, occurs so that the points $N_{i,1}$ and $N_{i,2}$ created near the point $\overline{N}_i$ return toward $\overline{N}_i$ and merge in it, and a stable 6-cycle survives (see the qualitative representation of the bifurcation in Fig. 11). Thus, the attractors are again two symmetric cycles of period 6, but the homoclinic bifurcations of s correspond to global bifurcations in the structure of the basins, due to the existence of a strange repellor. An example is given in Fig. 12, for $\beta = 0.261$, we can see that the structure of the basins of attraction of the 6-cycles N and N' are very complicated with a fractal chaotic structure, and the boundary $\mathscr{F}$ is an invariant set for T_2, on which the restriction of the map is chaotic. This fact shows how a system may have globally a complex structure in the basins, even in presence of simple attractors. When the structure of the basins becomes so complicated (really chaotic), it is difficult to know if an initial condition belongs to a basin of attraction or to another one. This fact leads to a kind of uncertainty because given an initial condition, we cannot easily foresee which attractor the system will reach, and small

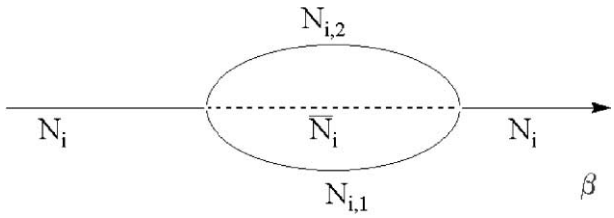

Fig. 11. Qualitative diagram representing the flip-bifurcation, also called period-doubling, followed by a period-halving.

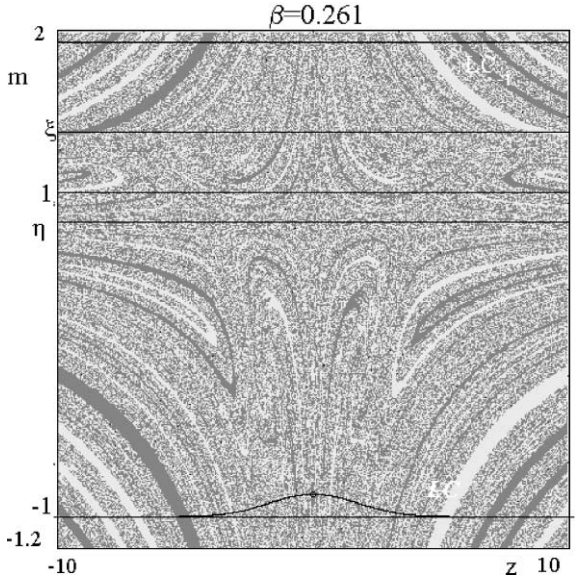

Fig. 12. Dark grey and white points belong to the basins of two symmetric 6-cycles of T_2.

perturbations in the initial conditions near the frontier of the basins can produce changes in the behaviour of the system as convergence to different sets.

As β continue to increase the 6-cycle node will merge with the saddle by saddle-node bifurcation and this "periodic window" on Γ closes, leaving for the map T_2 only one attractor, i.e. the invariant set Γ, on which there are quasiperiodic orbits.

3.4. Homoclinic bifurcation leading to a chaotic attractor

As the parameters β is further increased, the two closed sets Γ_1 and Γ_2 constituting Γ increase in size and approach the vertical axis $z = 0$. Clearly a global bifurcation shall occur when the two components shall merge, which is the object of the present subsection. The transition from a regular attractor to a chaotic one usually appears in a gradual way, through a sequence of bifurcations, but in the example we are considering in our map T_2, this transition instantaneously occurs in connection with the first homoclinic bifurcation of the saddle fixed point S^*. When the invariant set Γ is made up of two disjoint curves, the unstable manifold of the saddle S^* is given by two branches issuing symmetrically from the point and converging toward the components Γ_1 and Γ_2 so that the closure of $W^U(S^*)$ includes Γ. $W^S(S^*)$ is given by ω_0 (the vertical axis $z = 0$), ω_{-1} (the line $m = \eta$), and all the preimages of ω_{-1}. But as long as Γ_1 and Γ_2 are disjoint we have $W^S(S^*) \cap W^U(S^*) = \emptyset$, that is, no homoclinic point of S^* exists. In the example we are investigating, the contact occurs for $\beta^* \simeq 0.275289$. As shown in Fig. 13 the two pieces Γ_1 and Γ_2 have two contact points on the line $z = 0$: the point A and its image, the fixed point S^*. We note that this contact bifurcation corresponds to the appearance of the first homoclinic orbit of the saddle S^*, so that we call it homoclinic bifurcation of S^*. In fact, the point A belongs to ω_0 and is mapped by the map T_2 into S^*, so that the forward orbit of A goes to S^*, and we can see that also a sequence of preimages of A exists, approaching S^*, giving an homoclinic orbit of S^*, in a situation of "tangency" of $W^S(S^*)$ and $W^U(S^*)$. The two rank-1 preimages of A are the points $T^{-1}(A) = A_{-1,L} \cup A_{-1,R}$ belonging to ω_{-1}, and among the two preimages of $A_{-1,L}$ (respectively $A_{-1,R}$) at least one belongs to the closed set $\Gamma = \Gamma_1 \cup \Gamma_2$ which is now $W^U(S^*)$ and so on iteratively, sequences of preimages of $A_{-1,L}$ (respectively $A_{-1,R}$) approach S^* on both sides. Clearly for $\beta > \beta^*$ we expect the appearance of transverse intersections between $W^S(S^*)$ and $W^U(S^*)$, and in fact these appear. For example, the points A and B on the line ω_0 ($z = 0$) in Fig. 14a are homoclinic points of S^* belonging to two different homoclinic orbits, and many other exist. When $\beta > \beta^*$ the attractor suddenly becomes a closed invariant set (see Fig. 14a) with a chaotic structure. Let us denote with γ_L and γ_R two symmetric arcs of the attractor which cross the line $m = \eta$ and let us call $A_{-1,L}$, $B_{-1,L}$ the contact points between γ_L and the line $m = \eta$. In a symmetric way we indicate by $A_{-1,R}$, $B_{-1,R}$ the intersections of the same line with γ_R. It is clear that

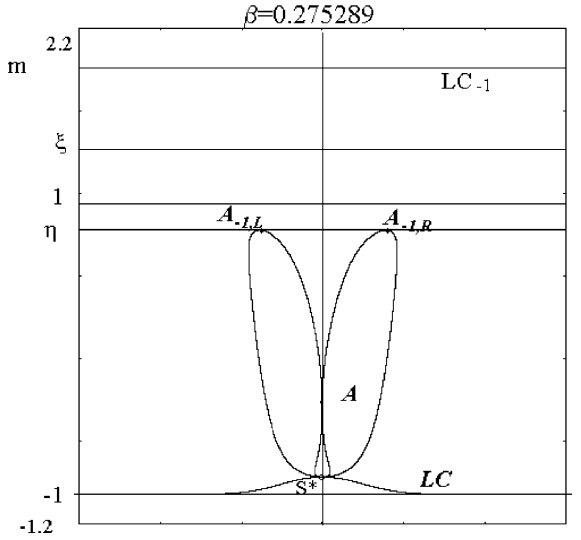

Fig. 13. Contact bifurcation: Γ_1 and Γ_2 merge in the point A and in the fixed point S^*.

$$T_2(A_{-1,L}) = T_2(A_{-1,R}) = A$$

and

$$T_2(B_{-1,L}) = T_2(B_{-1,R}) = B$$

Moreover the points to the left of $z = 0$ are mapped into points located on the right of $z = 0$ and viceversa, therefore $T_2(\gamma_L)$ is an arc placed on the right of $z = 0$ (see Fig. 14a) and $T_2(\gamma_R)$ is an arc on the left of $z = 0$ both crossing through A and B. As A and B belong to ω_0 and their image is S^*, $T_2^2(\gamma_L)$ is an arc, or loop, issuing from S^* belonging to the half plane $z < 0$, $T_2^2(\gamma_R)$ is the symmetrical arc as shown in the enlargement in Fig. 14b. And so on, $T_2^3(\gamma_L)$ is a loop issuing from S^* located in $z > 0$, $T_2^3(\gamma_R)$ is the symmetrical arc, and the further iterations give rise to stretched loops issuing from S^* that are quite long and reach the line $m = \eta$, with arcs under γ_L and γ_R. For these arcs the mechanism of the images is also repeated. It is clear that from the fixed point S^* infinitely many arcs, $T_2^n(\gamma_L)$ and $T_2^n(\gamma_R)$ for $n \geqslant 2$ exist and many other arcs cross $m = \eta$ whose images produce infinitely many arcs issuing from S^* etc., this self-similar mechanism is repeated, creating an attractor with fractal structure which is a chaotic attractor that we can identify with the closure of $W^U(S^*)$.

3.5. Feasible region

We recall that in our model z represents the deviation of the expected value from the equilibrium price p^* i.e.

$$z_t = p^e_{t+1} - p^*$$

and from an economic point of view the model is meaningful only if

$$p^e = z + p^* > 0$$

that is, for

$$z > -p^* = -\frac{A}{B+b} \tag{30}$$

We note however that differently from what occurs in invertible maps the line $z = -p^*$ is not the only boundary which must be taken under control in order to have the region, R say, of feasible trajectories. In fact, such a region R is a portion of the plane bounded by the line $z = -p^*$ and all its preimages of any rank, and being T_2 noninvertible, this set includes something else besides $z = -p^*$. In order to show that this set, say ∂R, may be involved in some bifurcation we shall consider a different set of fixed parameter:

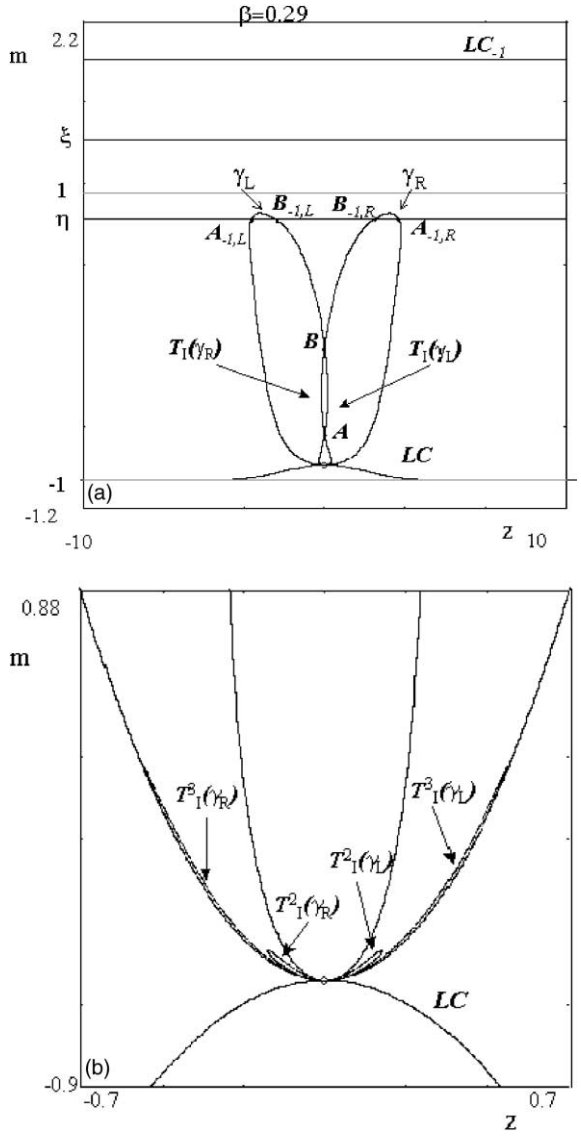

Fig. 14. Chaotic attractor which follows the homoclinic bifurcation of S^*.

$$C_1 = 40, \quad C_2 = 5, \quad \alpha = 0.6, \quad b = 1.5, \quad B = 0.3, \quad A = 15 \tag{31}$$

which allows us to show a contact bifurcation between the chaotic attractor and the boundary of the feasible region ∂R. In Fig. 15a we show a chaotic attractor which follows the homoclinic bifurcation of S^*, as described in the previous subsection. The unfeasible trajectories are represented in grey and the boundary of that region, ∂R, is given by the line $z = -p^*$ and its preimages. As β increases, we see from Fig. 15b that the boundary of this region approaches the chaotic attractor, and *tongues* from the region Z_0 are close to Z_2. Thus bifurcations in the structure of the feasible set are expected to occur. In fact, as we can see from Fig. 15c, the contact bifurcation gives rise to islands of grey points, so that the simply connected feasible region R (made up of the light grey points in Fig. 15) becomes a multiply connected region (i.e. a connected region with holes). From Fig. 15c we can see that the grey region is now very close to the chaotic set in the feasible region. A contact between the chaotic attractor and ∂R will denote the end for our applicative interpretation, because after this contact the generic trajectory will have negative values in the expected prices in an unpredictable way. We remark that this is a different kind of bifurcation, not related to the dynamic model from a mathematical point of view, but only to its economic meaning.

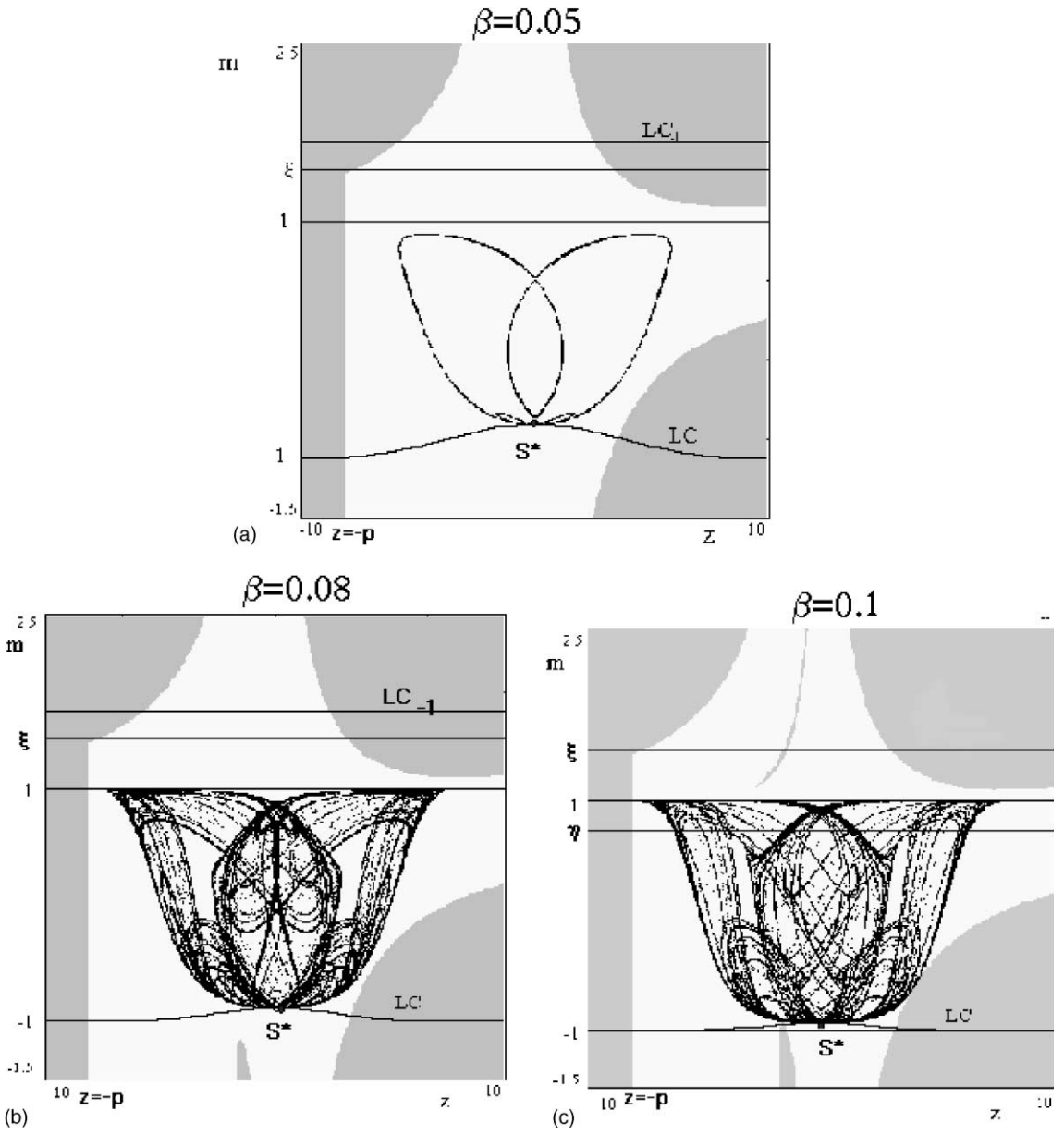

Fig. 15. $C_1 = 40$, $C_2 = 5$, $\rho = 0.4$, $b = 1.5$, $B = 0.3$, $A = 15$.

Acknowledgements

The authors want to thank Cars Hommes for valuable suggestions which motivated the present work. This work has been performed under the activity of the national research project "Nonlinear Dynamics and Stochastic Models in Economics and Finance" MURST, Italy.

References

[1] Birkhoff GD, Smith P. Structure analysis of surface transformations. Journal de Mathematique 1928;S9(7):345–79.
[2] Bischi GI, Gardini L. Basin fractalization due to focal points in a class of triangular maps. Int J Bifurcat Chaos 1997;7:1555–77.

[3] Bischi GI, Gardini L, Mira C. Maps with denominator. Part 1: some generic properties. Int J Bifurcat Chaos 1999;9:119–53.
[4] Brock WA, Hommes CH. Rational route to randomness. Discussion Paper Tinbergen Institute, Amsterdam, 1995.
[5] Brock WA, Hommes CH. A rational route to randomness. Econometrica 1997;65(5):1059–95.
[6] Brock WA, Hommes CH. Models of complexity in economics and finance. In: Heij C et al., editors. System Dynamics in Economic and Financial Models. John Wiley; 1997.
[7] Brock WA, Hommes CH. Heterogeneous beliefs and routes to chaos in a simple asset pricing model. J Econom Dyn Control 1998;22:1235–74.
[8] Chiarella C, Dieci R, Gardini L. Asset price dynamics in a financial market with fundamentalists and chartists. Discrete Dyn Nat Soc 2001;6:69–99.
[9] Chiarella C, He XZ. Heterogeneous beliefs, risk and learning in a simple asset pricing model. Comput Eco, forthcoming.
[10] Delli Gatti D, Gallegati M, Kirman A, editors. Market Structure, Aggregation & Heterogeneity. Cambridge University Press; 2000.
[11] De Vilder R. Complicated endogenous business cycles under gross substitutability. J Econom Theory 1996;71:416–42.
[12] De Vilder R. On the transition from local regular to global irregular fluctuations. J Econom Dyn Control 2000;24:247–72.
[13] Foroni I. Meccanismi di apprendimento in mercati omogenei ed eterogenei, Ph.D. Thesis, 2001.
[14] Frouzakis CE, Gardini L, Kevrekidis IG, Millerioux G, Mira C. On some properties of invariant sets of two-dimensional noninvertible maps. Int J Bifurcat Chaos 1997;7:1167–94.
[15] Gardini L. Homoclinic bifurcations in *n*-dimensional endomorphisms, due to expanding periodic points. Nonlinear Anal 1994;23(8):1039–89.
[16] Lux T. Herd behaviour, bubbles and crashes. Econom J 1995;105:881–96.
[17] Mira C. Chaotic dynamics. From the one-dimensional endomorphism to the two-dimensional diffeomorphism. Singapore: World Scientific; 1987.
[18] Mira C, Fournier-Prunaret D, Gardini L, Kawakami H, Cathala JC. Basin bifurcations of two-dimensional noninvertible maps: fractalization of basins. Int J Bifurcat Chaos 1994;4(2):343–81.
[19] Mira C, Gardini L, Barugola A, Cathala JC. Chaotic dynamics in two-dimensional noninvertible maps. Singapore: World Scientific; 1996.
[20] Gavrilov NK, Shilnikov LP. On three dimensional dynamical systems close to systems with structurally unstable homoclinic curve I. Mat USSR Sbornik 1972;17:467–85.
[21] Gavrilov NK, Shilnikov LP. On three dimensional dynamical systems close to systems with structurally unstable homoclinic curve II. Mat USSR Sbornik 1972;19:139–56.
[22] Wiggins S. Global bifurcations and chaos analytical methods. New York: Springer Verlag; 1988.